

Distributed Synchrony in a Cell Assembly of Spiking Neurons

Nir Levy David Horn

School of Physics and Astronomy

Tel Aviv University Tel Aviv 69978, Israel

Isaac Meilijson Eytan Ruppin

School of Mathematical Sciences,

Tel Aviv University Tel Aviv 69978, Israel

February 18, 2001

Abstract

We investigate the formation of a Hebbian cell assembly of spiking neurons, using a temporal synaptic learning curve that is based on recent experimental findings. It includes potentiation for short time delays between pre- and post-synaptic neuronal spiking, and depression for spiking events occurring in the reverse order. The coupling between the dynamics of synaptic learning and that of neuronal activation leads to interesting results. One possible mode of activity is distributed synchrony, implying spontaneous division of the Hebbian cell assembly into groups, or subassemblies, of cells that fire in a cyclic manner. The behavior of distributed synchrony is investigated both by simulations and by analytic calculations of the resulting synaptic distributions.

1 Introduction

Consider the process of formation of a Hebbian cell assembly. Conventional wisdom would proceed along the following line of reasoning: start out with a group of neurons that are interconnected, using both excitatory and inhibitory cells. Feed them with a common input that is strong enough to produce action potentials, and let the excitatory synapses grow until a consistent firing pattern can be maintained even if the input is turned off. Using theoretical models of neuronal and synaptic dynamics we follow this procedure and study the resulting firing modes. Although the model equations may be an oversimplification of true biological dynamics, the emerging firing patterns are intriguing and may connect to existing experimental observations.

Recent studies of firing patterns by Brunel (1999) have shown in simulations, and in mean-field calculations, that large scale sparsely connected neuronal networks can fire in different modes. Whereas strong excitatory couplings lead to full synchrony, weaker couplings will usually lead to asynchronous firing of individual neurons that can exhibit either oscillatory or non-oscillatory collective behavior. For fully connected networks there exists evidence of the possibility of cluster formations, where the different neurons within a cluster fire synchronously. This phenomenon was analyzed by Golomb *et al.* (1992) in a network of phase-coupled oscillators, and was studied in networks of pulse-coupled spiking neurons by van Vreeswijk (1996) and by Hansel *et al.* (1995).

In contrast to previous studies, the present investigation concentrates on the study of a network storing patterns via Hebbian synapses. We mainly concentrate on a single Hebbian cell-assembly, where full connectivity is assumed between all excitatory neurons. We employ synaptic dynamics that are based on the recent experimental observations of Markram *et al.* (1997) and Zhang *et al.* (1998). They have shown that potentiation or depression of synapses connecting excitatory neurons occurs only if both pre- and post-synaptic neurons

fire within a critical time window of approximately 20ms. If the pre-synaptic neuron fires first, potentiation will take place. Depression is the rule for the reverse order. The regulatory effects of such a synaptic learning curve on the synapses of a single neuron that is subjected to external inputs were investigated by Song *et al.* (2000) and by Kempter *et al.* (1999). We investigate here the effect of such a rule within an assembly of neurons that are all excited by the same external input throughout a training period, and are allowed to influence one another through their resulting sustained activity. We find that this synaptic dynamics facilitates the formation of clusters of neurons, thus splitting the Hebbian cell-assembly into subassemblies and producing the firing pattern that we call *distributed synchrony* (DS).

In the next section we present the details of our model. It is based on excitatory and inhibitory spiking neurons. The synapses among excitatory neurons undergo learning dynamics that follow an asymmetric temporal rule of the kind observed by Markram *et al.* (1997) and Zhang *et al.* (1998). We study the resulting firing patterns and synaptic weights in sections 3 and 4. The phenomenon of distributed synchrony is displayed and discussed. To understand it better, we perform in sections 5 and 6 a theoretical analysis of the influence of an ordered firing pattern on the development of the synaptic couplings. This is derivable in a two-neuron model, and is compared with the results of simulations on a network of neurons. In section 7 we proceed to demonstrate that similar types of dynamics may appear also in the presence of multiple memory states. A first version of our model was presented at Horn *et al.* (2000).

2 The Model

We study a network composed of N_E excitatory and N_I inhibitory integrate-and-fire neurons. Each neuron in the network is described by its subthreshold membrane potential $V_i(t)$

obeying

$$\dot{V}_i(t) = -\frac{1}{\tau_n}V_i(t) + RI_i(t) , \quad (1)$$

where τ_n is the neuronal membrane decay time constant. A spike is generated when $V_i(t)$ reaches the threshold θ , upon which a refractory period of τ_R sets in and the membrane potential is reset to V_{reset} where $0 < V_{reset} < \theta$. For simplicity we set the level of the rest-potential to 0. $I_i(t)$ is the sum of recurrent and external synaptic current inputs. The net synaptic input charging the membrane of *excitatory* neuron i at time t is:

$$RI_i(t) = \sum_j^{N_E} w_{ij}(t) \sum_l \delta(t - t_j^l - \tau_{dij}) - \sum_k^{N_I} J_{ik}^{EI} \sum_m \delta(t - t_k^m - \tau_{dik}) + I^E , \quad (2)$$

summing over the different synapses of $j = 1, \dots, N_E$ excitatory neurons and of $k = 1, \dots, N_I$ inhibitory neurons, with synaptic efficacies $w_{ij}(t)$ and J_{ik}^{EI} respectively. The sum over l (m) represents a sum on different spikes generated at times t_j^l (t_k^m) by the respective neurons j (k). I^E , the external current, is assumed to be random and independent at each neuron and each time step, drawn from a Poisson distribution.

Similarly, the synaptic input to the *inhibitory* neuron i at time t is

$$RI_i(t) = \sum_j^{N_E} J_{ij}^{IE} \sum_l \delta(t - t_j^l - \tau_{dij}) - \sum_k^{N_I} J_{ik}^{II} \sum_m \delta(t - t_k^m - \tau_{dik}) + I^I , \quad (3)$$

where I^I is the external current.

We assume full connectivity among the excitatory neurons, but only partial connectivity for all other three types of possible connections, with connection probabilities denoted by C^{EI} , C^{IE} and C^{II} . In the following we will report simulation results in which the synaptic delays τ_d were assigned to each synapse, or pair of neurons, randomly, chosen from some finite set of values. Our analytic calculation will be done for one single value of the synaptic delay parameter.

Synaptic efficacies between two excitatory neurons, w_{ij} , are potentiated or depressed according to the temporal firing patterns of the pre- and post-synaptic neurons. Other

synaptic efficacies, namely those involving at least one inhibitory neuron, J^{EI} , J^{IE} and J^{II} , are assumed to be constant. Each excitatory synapse obeys

$$\dot{w}_{ij}(t) = -\frac{1}{\tau_s}w_{ij}(t) + F_{ij}(t) , \quad (4)$$

where we allowed for a synaptic decay constant τ_s . We will discuss situations where it is infinite, but consider also cases when it is finite but larger than the membrane time constant τ_n . $w_{ij}(t)$ are constrained to vary in the range $[0, w_{max}]$. The change in synaptic efficacy is defined by

$$F_{ij}(t) = \sum_{k,l} \left[\delta(t - t_i^k) K_P(t_j^l - t_i^k) + \delta(t - t_j^l) K_D(t_j^l - t_i^k) \right] , \quad (5)$$

where K_P and K_D are the potentiation and depression branches of a kernel function.

Following Markram *et al.* (1997) and Zhang *et al.* (1998) we distinguish between the situation where the postsynaptic spike, at t_i^k , appears after or before the presynaptic spike, at t_j^l . This distinction is made by the use of asymmetric kernel functions that capture the essence of the experimental observations.

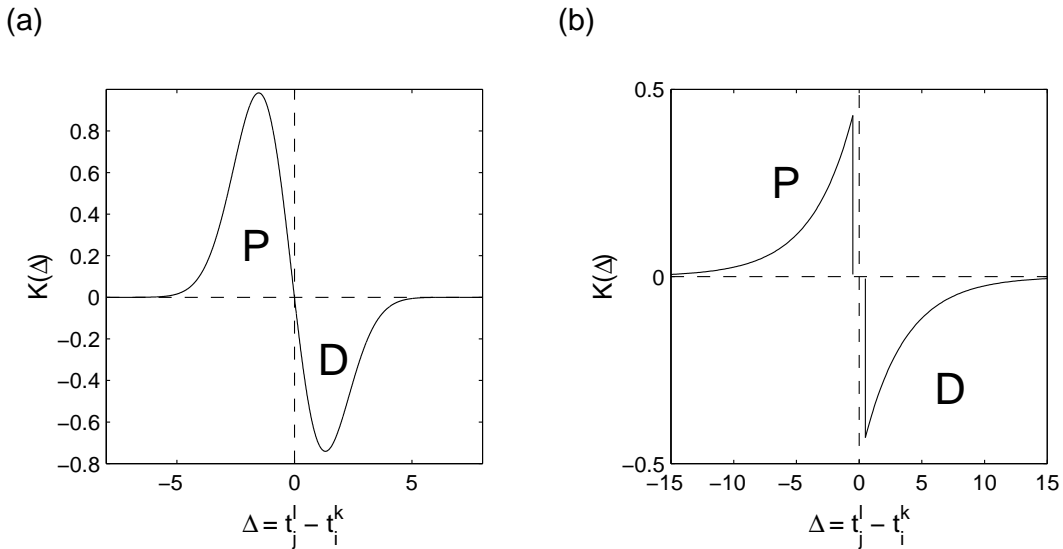


Figure 1: Two choices of the kernel function whose left part, K_P , leads to potentiation of the synapse, and whose right branch, K_D , causes synaptic depression.

Figure 1 displays the two kernel functions that are used for analysis and simulations: a continuous function

$$K_1(\Delta) = -c\Delta \exp \left[- (a\Delta + b)^2 \right] \quad (6)$$

as plotted in Figure 1(a), and a discontinuous function

$$K_2(\Delta) = \begin{cases} K_P(\Delta) = a \exp [c\Delta] & \text{if } \Delta < -\epsilon \\ K_D(\Delta) = -b \exp [-c\Delta] & \text{if } \Delta > \epsilon \\ 0 & \text{otherwise} \end{cases} \quad (7)$$

plotted in Figure 1(b). For both kernels the constants a, b, c change the span, asymmetry and strength of the kernels. In the discontinuous kernel ϵ sets the minimal phase shift that the kernel is sensitive to. The shapes of the kernels were determined so that their time windows match the typical inter-spike-intervals of the excitatory neurons, characteristically between 10ms to 30ms in the simulations that we will report below. As a result the span of the kernel is somewhat smaller than the experimentally observed ones. In future more realistic neuronal dynamics one should aim for both larger time-span of the kernel and lower sustained firing rates of excitatory neurons, thus getting closer to experimental observations.

It should be noted that the synaptic dynamics of Eq. (4) do not include short-term synaptic depression due to high frequency of presynaptic neuronal firing, such as in Markram and Tsodyks (1996) and Abbott *et al.* (1997). Neither do the neuronal dynamics include neuronal regulation, a mechanism proposed by Horn *et al.* (1998) and termed synaptic scaling by Turrigiano *et al.* (1998) who observed it experimentally. These two types of effects (see the recent review by Abbott and Nelson (2000)) should be added to the spike-timing dependent synaptic plasticity (STDP) that is studied here. In the present paper we study the interplay of STDP with simple integrate-and-fire neuronal dynamics. We limit ourselves to only part of synaptic and neuronal dynamics in order to be able to discern specific trends and obtain new qualitative results. The latter will have then to be studied in improved, more biological, models.

3 Dynamical Attractors in Hebbian Assemblies

We start by studying the behavior of the network described in the last Section using numerical simulations. We look at the types of dynamical attractors the excitatory network flows into, starting from random firing induced by stochastic inputs. We find that in addition to synchronous and asynchronous dynamical attractors, a mode of *distributed synchrony* (DS) emerges. In this state, the network breaks into n groups, or subassemblies, of neurons, each of which fires synchronously.

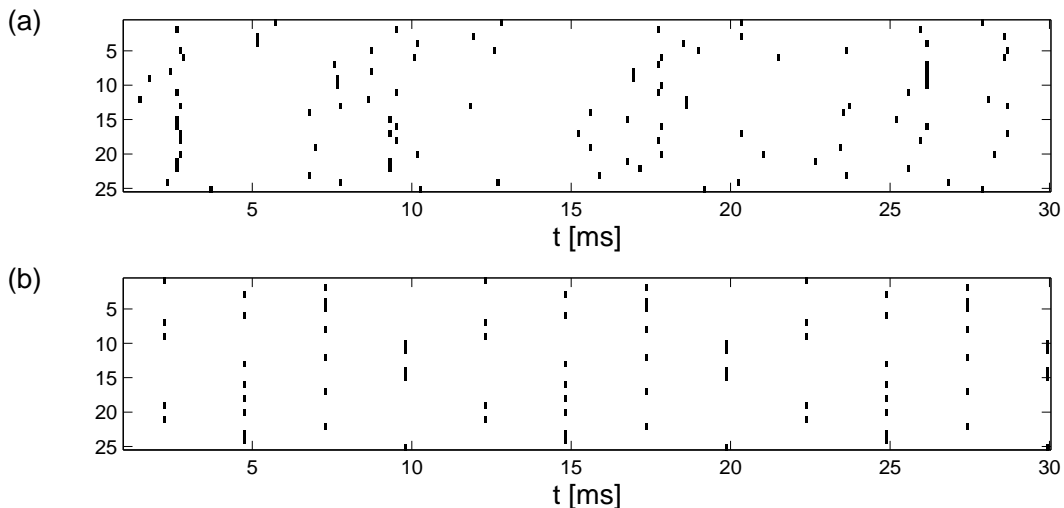


Figure 2: Two firing patterns observed in a network of excitatory and inhibitory integrate and fire neurons. A raster plot of 25 out of N_E neurons is shown. (a) Asynchronous firing mode in a network of $N_E = 100$. (b) 4-cycle distributed synchrony mode in a network of $N_E = 50$. These simulations used the continuous kernel and common synaptic delay $\tau_d = 2.5$ ms. Each dot corresponds to the firing of a spike by one excitatory neuron. The simulation time step was 0.1ms.

Figure 2(a) shows an example of asynchronous firing and Figure 2(b) shows a distributed synchrony mode which forms a 4-cycle. These modes of firing emerge *spontaneously* as an outcome of the neuronal and synaptic dynamics. The synaptic efficacies w_{ij} are taken to be initially random and small. The firing dynamics induced by the external input change the

synaptic efficacies so that some concentrate near the upper bound and some near zero. In Figure 3 we show the excitatory synaptic matrices that correspond to the patterns of firing presented in Figure 2.

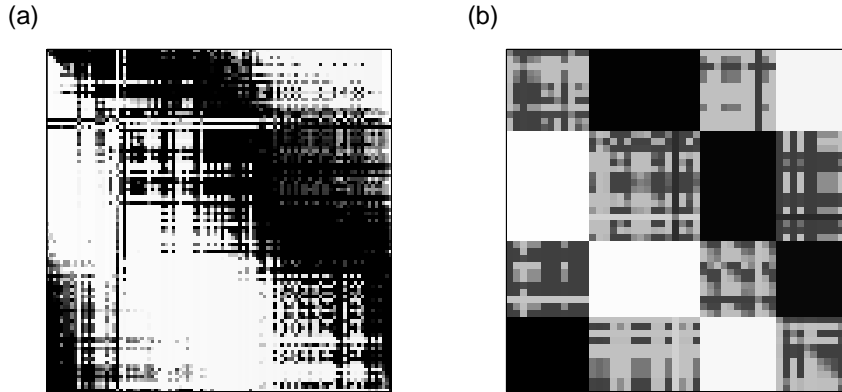


Figure 3: The excitatory synaptic matrices, of sizes $N_E \times N_E$ that were created by the dynamics that led to the firing patterns shown in Figure 2. (a) The synaptic matrix when the excitatory neurons fire asynchronously. (b) The 4-cycle synaptic matrix. The gray scale shading represents the magnitude of the synapses: with white representing the upper bound and black the lower bound.

The synaptic matrices shown in Figure 3 are displayed in a basis that corresponds to the order of firing of the neurons. Thus we obtain a clear block structure for the case of distributed synchrony in Figure 3(b). The off diagonal strong couplings signify that each coherent group of neurons feeds the activity of groups that follow it. This block form is absent when the network fires asynchronously, as shown in Figure 3(a).

In all simulations we tested networks of $N_E = 50$ or 100 excitatory neurons and $N_I = 50$ inhibitory neurons. J^{EI} and J^{II} were chosen to be 0.5 and J^{IE} was 0.5 for $N_E = 50$ and 0.25 for $N_E = 100$. C^{EI} , C^{IE} and C^{II} were taken to be 0.5 . τ_n was chosen to be 10ms for the excitatory and inhibitory neurons. The threshold parameter θ was 20mV , V_{reset} was 10mV and the refractory period τ_R was set to 2ms . The external inputs to the excitatory and inhibitory neurons were Poisson generated with averages of $\langle I^E \rangle = \lambda_E$ and $\langle I^I \rangle = \lambda_I$.

Turning the excitatory external input currents off or decreasing their magnitude after a while, led to sustained firing activity in the range of 80-150 Hz. The firing frequencies depended on the dynamical state the system flows into. For instance, the mean firing rate was kept approximately 130Hz in a 3-cycle mode and 100Hz in a 4-cycle for a common synaptic delay of 2.5ms. The synaptic decay constant τ_s was taken to be larger than 100ms. w_{max} was set to 1 when $N_E = 50$ and to 0.5 when $N_E = 100$.

4 Stability of a Cycle

A stable DS cycle can be simply understood when a single synaptic delay sets the basic step, or phase difference, of the cycle. When several delay parameters exist, a situation that probably more accurately represents the α -function character of synaptic transmission in cortical networks, distributed synchrony may still be obtained. In this case, however, the cycle may destabilize and regrouping may occur by itself as time goes on, because different synaptic connections that have different delays can interfere with one another. Nonetheless, over time scales of tens of milliseconds grouping is stable. Figure 4 shows such behavior.

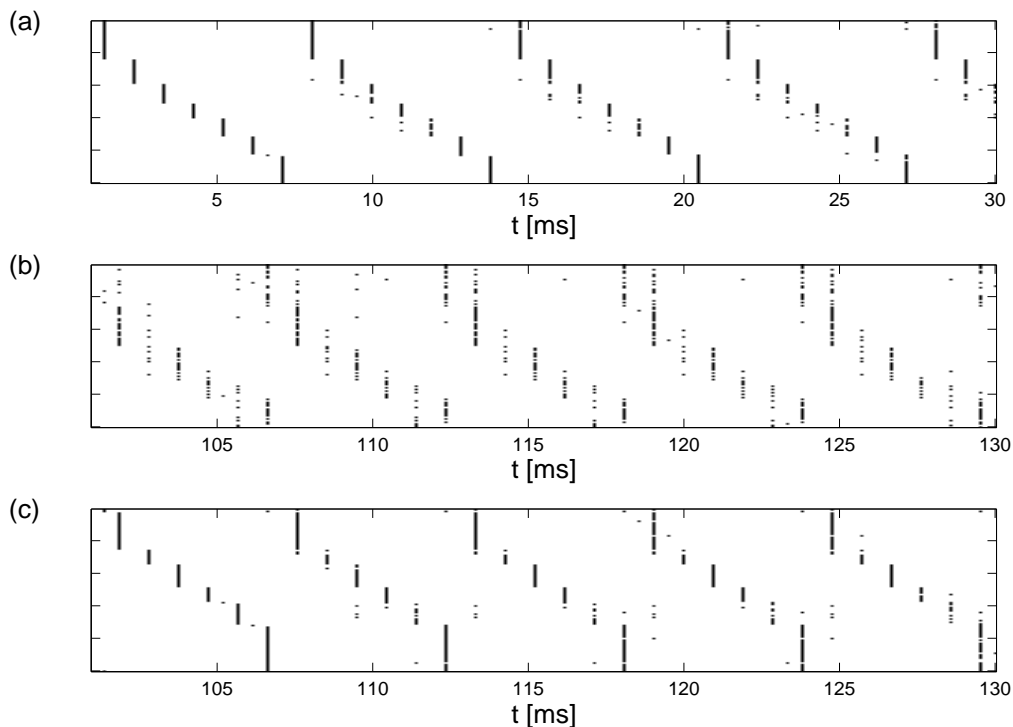


Figure 4: Raster plot of $N_E = 100$ neurons displaying unstable distributed synchrony. (a) Coherent groups of neurons are formed by synaptic dynamics with discontinuous kernel function ($a = 0.075$, $b = 0.05$, $c = 1.2\text{ms}^{-1}$, $\epsilon = 0.5\text{ms}$ and $\tau_s = \infty$) (b) This grouping structure changes gradually after 100ms or so. (c) The data of (b) are redisplayed in a new basis showing that regrouping of distributed synchrony took place. The synaptic delays were randomly chosen to be either 1, 2, or 3ms.

5 The Two-Neurons Synaptic Matrix

The values of synaptic connections between excitatory neurons are governed by the kernel function $K(t_j^l - t_i^k)$ and by the temporal firing patterns of the two neurons. In this section the synaptic matrix of a two-neuron system is analyzed in terms of these variables. We look at neurons i and j and at the synaptic connections w_{ij} and w_{ji} between them. The stationary joint density function $f(w_{ij}, w_{ji})$ of the two synaptic connections is calculated. This function is the probability of finding synaptic connections w_{ij} and w_{ji} between the

pair of neurons when the system is in its steady state. The neurons are assumed to fire with frequency $\nu(t)$ keeping a phase shift $\eta(t)$ between their firing times. Although we allow for these two variables to be time dependent, we will look for stationary solutions.

The dynamics are described in a two-dimensional vector form, where Eq. 4 is rewritten as:

$$\dot{\mathbf{W}}(t) = -\frac{1}{\tau_s}\mathbf{W}(t) + \mathbf{F}(t). \quad (8)$$

The boldface notation stands for the vectors

$$\mathbf{W}(t) = \begin{pmatrix} w_{ij}(t) \\ w_{ji}(t) \end{pmatrix}, \quad \mathbf{F}(t) = \begin{pmatrix} F_{ij}(t) \\ F_{ji}(t) \end{pmatrix}. \quad (9)$$

Eq. 8 describes the dynamic behavior of the synaptic matrix between the two neurons. The dynamics can be well approximated by a stochastic process in which the system, excited by stochastic inputs, is in a stable state of distributed synchrony. This approximation is valid under the following two assumptions. First, the firing pattern of the network is almost stable, that is, the frequency ν is constant in time and the phase shift $\eta(t)$ has small fluctuations. Second, the synaptic changes are slow compared to the neuronal firing rate. In this slow dynamics the number of contributions from $F_{ij}(t)$ during a synaptic integration time interval of the type used in our simulations may be estimated to be several tens, justifying the replacement of these contributions by a stochastic Gaussian process as follows.

Let us define the vector $\bar{\mathbf{F}}$ of means of $\mathbf{F}(t)$ and the covariance matrix \mathbf{C} of $\mathbf{F}(t)$

$$\bar{\mathbf{F}} = \begin{pmatrix} \mu_{F_{ij}} \\ \mu_{F_{ji}} \end{pmatrix}, \quad \mathbf{C} = \begin{pmatrix} \sigma_{F_{ij}} & \sigma_{F_{ij}}\sigma_{F_{ji}}\rho \\ \sigma_{F_{ij}}\sigma_{F_{ji}}\rho & \sigma_{F_{ji}} \end{pmatrix}, \quad (10)$$

where $\mu_{F_{ij}}$, $\mu_{F_{ji}}$, $\sigma_{F_{ij}}$, $\sigma_{F_{ji}}$ and ρ are the means, standard deviations and the correlation coefficient of $F_{ij}(t)$ and $F_{ji}(t)$. The detailed derivation of $\bar{\mathbf{F}}$ and \mathbf{C} is given in Appendix A. For this derivation $\eta(t)$ is assumed to have a stationary normal distribution with mean μ_η and standard deviation σ_η .

Under these assumptions, the stochastic process that approximates the synaptic dynamics of Eq. 8 satisfies the Fokker-Planck equation for the joint density $f(\mathbf{W}, t)$ (see Gardiner (1985)),

$$\frac{\partial f(\mathbf{W}, t)}{\partial t} = -\nabla \cdot \mathbf{J}(\mathbf{W}, t), \quad (11)$$

where the probability current $\mathbf{J}(\mathbf{W}, t)$ is defined in terms of the *drift vector*

$$\mathbf{A}(\mathbf{W}, t) = \bar{\mathbf{F}} - \frac{1}{\tau_s} \mathbf{W}(t) \quad (12)$$

as

$$J_l(\mathbf{W}, t) = A_l(\mathbf{W}, t)f(\mathbf{W}, t) - \frac{1}{2} \sum_k C_{lk} \frac{\partial}{\partial W_k} f(\mathbf{W}, t). \quad (13)$$

The synaptic connections are free to vary within the range $[0, w_{max}]$, therefore we impose on Eq. 11 reflecting boundary conditions: $\mathbf{n} \cdot \mathbf{J}(\mathbf{W}, t) = 0$, where \mathbf{n} is a unit vector normal to the boundary surface. The stationary solution $f(\mathbf{W})$ for which the probability current vanishes for all \mathbf{W} within the range implies $\mathbf{J}(\mathbf{W}) = 0$. The solution is

$$f(\mathbf{W}) = \mathcal{N} \exp \left[\mathbf{W}^T \mathbf{C}^{-1} \mathbf{A}(\mathbf{W}) + \mathbf{W}^T \mathbf{C}^{-1} \bar{\mathbf{F}} \right] \quad (14)$$

where \mathcal{N} normalizes $f(\mathbf{W})$. This probability density is a function of three free parameters characterizing the stationary pattern of firing of neurons i and j : the frequency ν the mean μ_η of the phase shift and its variance σ_η^2 . Figure 5 displays three specific realizations of $f(\mathbf{W})$.

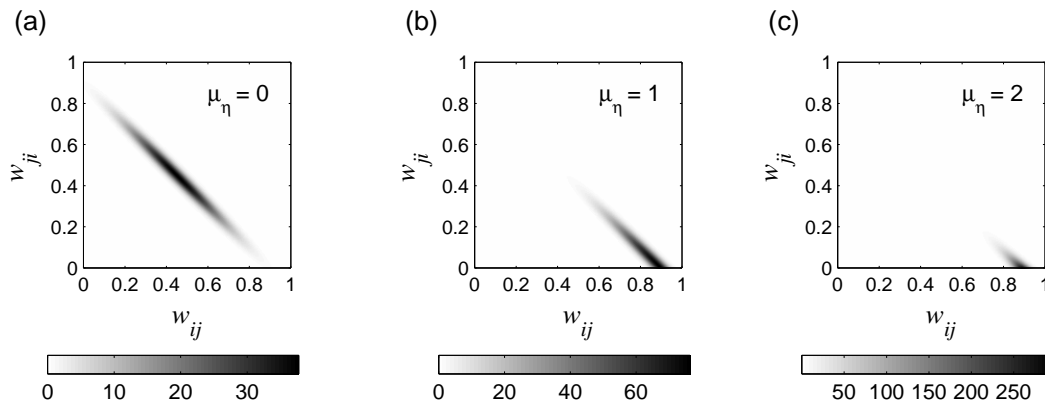


Figure 5: The stationary joint density function $f(\mathbf{W})$ is calculated for the kernel described in Eq. 6, where $a = 0.2\text{ms}^{-1}$, $b = 0.1$ and $c = 0.6$. Other parameters are: $\nu = 125\text{Hz}$, $\sigma_\eta = 5$, $\tau_s = 250\text{ms}$, $w_{max} = 1$. The plotted density function is for: (a) $\mu_\eta = 0$, (b) $\mu_\eta = 1$ and (c) $\mu_\eta = 2$.

As evident from Figure 5 the stationary distribution of the synapses between neuron i and j is asymmetric when $\mu_\eta > 0$. This characteristic is seen in the simulations shown in Figure 3 and is a consequence of the asymmetric structure of the kernel function.

6 Analysis of a Cycle

As shown in the previous section, the phase shift between the firing times of two neurons characterizes their synaptic connections. These phase shifts are determined by the firing pattern of the network. By evaluating all of them, the synaptic distribution function for a network of N_E neurons can be constructed. Assessing all the phase shifts for an arbitrary firing state may be difficult but for the case of distributed synchrony, when these phase shifts take several distinct values, the derivation can be carried out.

The calculation of the density function of the $N_E \times N_E$ synaptic matrix is made in two steps. First, the marginal density function $f_{ij}(w)$ for $w = w_{ij}$ is calculated. Then, the specific phase shifts are determined and the full distribution is constructed.

The marginal stationary distribution of w_{ij} is calculated under the same assumptions made in the previous section. The one dimensional Fokker-Planck equation for the probability density function f_{ij} of w_{ij} is

$$\frac{\partial f_{ij}(w, t)}{\partial t} = -\frac{\partial}{\partial w} \left[\left(\mu_{F_{ij}} - \frac{1}{\tau_s} w \right) f_{ij}(w, t) \right] + \frac{\sigma_{F_{ij}}^2}{2} \frac{\partial^2 f_{ij}(w, t)}{\partial w^2} \quad (15)$$

with reflecting boundary conditions imposed by the synaptic bounds, 0 and w_{max} . The resulting stationary density function satisfying $\frac{\partial f_{ij}(w, t)}{\partial t} = 0$ is

$$f_{ij}(w) = \frac{\mathcal{N}}{\sigma_{F_{ij}}^2} \exp \left[\frac{1}{\sigma_{F_{ij}}^2} \left(2\mu_{F_{ij}} w - \frac{1}{\tau_s} w^2 \right) \right] \quad (16)$$

where \mathcal{N} normalizes $f_{ij}(w)$. Note that for $\tau_s = \infty$ we obtain an exponential distribution which peaks at the upper bound w_{max} , or at the lower bound 0, depending on the sign of $\mu_{F_{ij}}$.

Eq. 16 expresses the stationary distribution of the synaptic efficacy between every presynaptic neuron j and postsynaptic neuron i in terms of variables that depend (see Appendix A) on the frequency ν and the phase shift parameters μ_η and σ_η . As an example, the case of a 3-cycle is solved for a network with a single synaptic delay τ_d . The mean firing frequency is taken to be $\nu = (3\tau_d)^{-1}$ with very little variations, assuming that the total synaptic current feeding a neuron in the next group to fire is large enough so that it will bring its membrane potential to the threshold almost regardless of its previous value. Thus, the phase shift between the firing time of each subassembly is τ_d and the period is n times this value. For $n = 3$, μ_η takes one of the values $-\tau_d, 0, \tau_d$. σ_η remains a free parameter reflecting the random noise introduced by the input I^E and by the coupled inhibitory network. Figure 6 presents the resulting structure of the synaptic matrix.

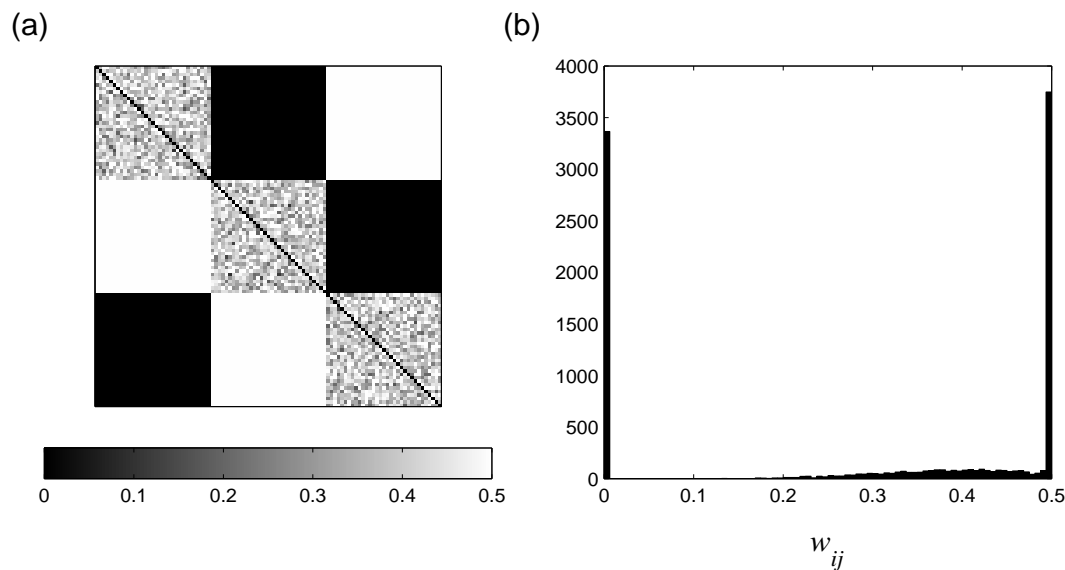


Figure 6: Results of the analysis for $n = 3$, $\sigma_\eta = 0.1\text{ms}$ and $\tau_d = 2.5\text{ms}$ under the continuous kernel function with $a = 0.5\text{ms}^{-1}$, $b = 0.1$, $c = 1$ and $\tau_s = 100\text{s}$. (a) The synaptic matrix. Each of the nine blocks symbolizes a group of connections between neurons that have a common phase shift μ_η . Values of w_{ij} are generated by Eq. 16 and represented by the gray scale tone. (b) The distribution of synaptic values between excitatory neurons.

This should be compared with Figure 7 which displays the results of a simulation of a system that converged to a 3-cycle DS. In this simulation we start out with $\tau_s = 100\text{ms}$ for the first 200ms using an input of $\lambda_E = 30$ which, after 200ms, is reduced to 20, while τ_s is elevated to 100s. $\lambda_I = 30$ during the first 200ms, and is reduced to 20 after that. We found that this procedure is useful to ensure fast convergence into a DS mode. As can be seen, the results obtained from the analysis are similar to those observed in the simulation. The main differences are in the diagonal blocks, where the analytic results have a flat distribution of synaptic weights due to $\mu_{F_{ij}}=0$ within such blocks, while the simulation results exhibit structure that develops in the course of the dynamical history of this matrix, including regrouping effects in unstable DS.

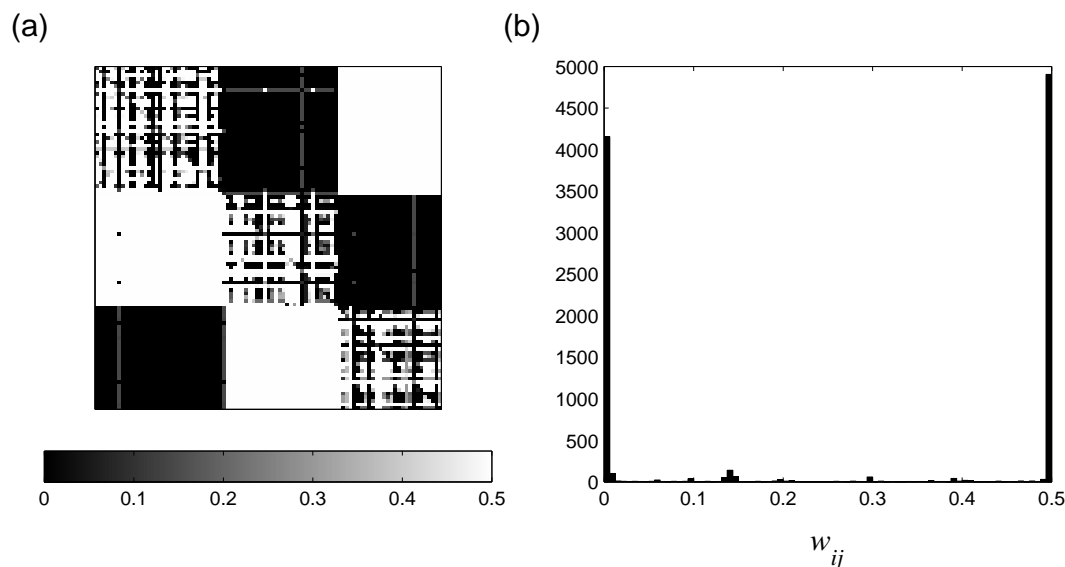


Figure 7: Simulation results for a network of $N_E = 100$ and $N_I = 50$ integrate-and-fire neurons, when the network is in a stable $n = 3$ DS state. $\tau_n = 10\text{ms}$ for both excitatory and inhibitory neurons. Other parameters are the same as in the previous figure. The average frequency of the neurons is approximately 130 Hz. (a) Gray scale representation of the synaptic matrix. (b) Histogram of the synaptic weights among excitatory neurons.

As evident from Figures 6 and 7 each group of neurons feeds the next one with synaptic efficacies that are as high as the upper synaptic bound, while low synaptic efficacies connect to neurons that belong to their own subassembly and zero connections exist with neurons in subassemblies that are activated prior to the group in question. This trait and the observed frequency of 130Hz confirms our assumption that $\nu = (3\tau_d)^{-1}$.

7 Overlapping Cell Assemblies

So far we have followed the procedure, stated at the beginning of the Introduction, of formation of a Hebbian cell-assembly. We noted that it can break into several subassemblies forming a cycle of DS. If such a cell-assembly should represent some memory in an associative memory model, we have to consider the problem of encoding of multiple memories. As a

first step toward answering this question we will show in this section that overlapping DS synaptic matrices can be employed in a retrieval problem.

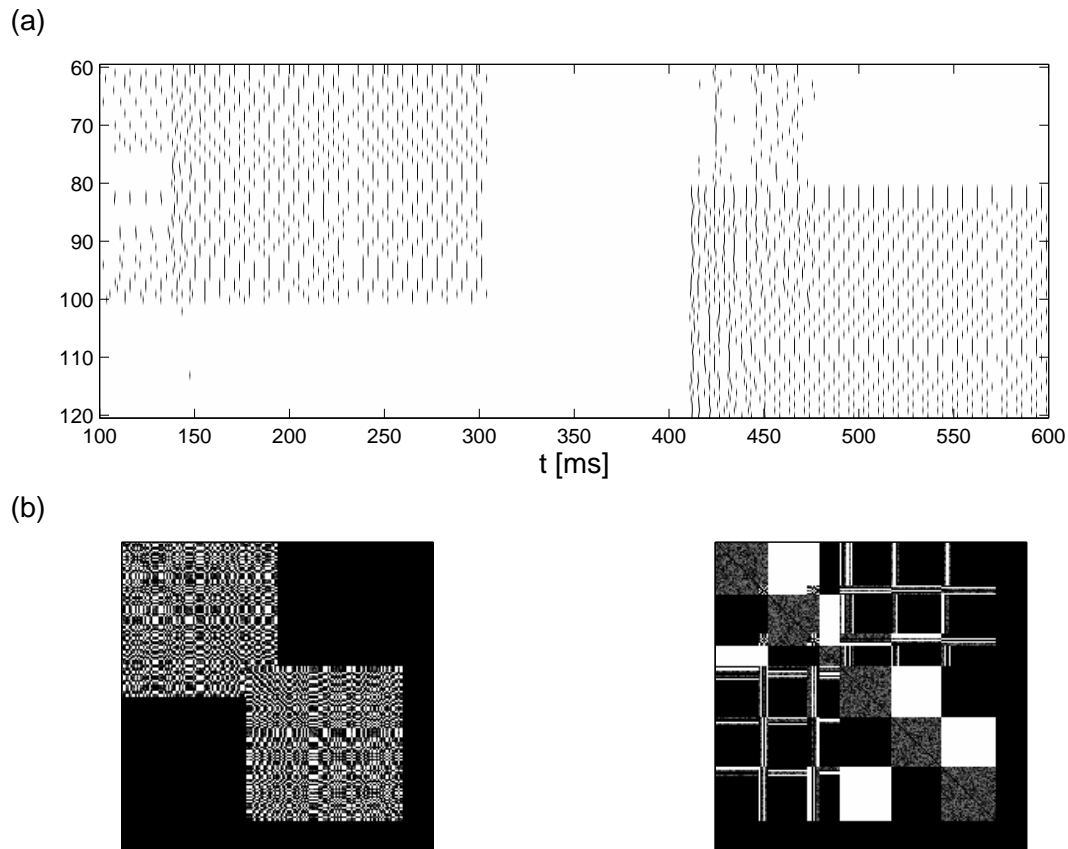


Figure 8: Memory retrieval of two overlapping cell assemblies. (a) Raster plot of the retrieval process. A subset of 60 neurons is shown, 40 belonging to each assembly, half of which belong to both. Each assembly fires in 3-cycle distributed synchrony. (b) The synaptic matrix, in a random order and in the order of neuronal firing. Each assembly is composed of 100 neurons out of $N_E = 200$. The overlap between the assemblies is 20%. In the retrieval process the excited assembly was given an input of $\lambda_E = 30$ for the first 150ms and $\lambda_E = 20$ afterwards, while the quiescent assembly receives $\lambda_E = 20$, which may be considered as background input. Other parameters were: $w_{max} = 0.5$, $N_I = 50$, and $\lambda_I = 20$, but for the period $300\text{ms} < t < 400\text{ms}$ where $\lambda_I = 30$.

Figure 8(a) presents the raster plot of a subset of the excitatory neurons during a retrieval

process with no active synaptic learning. The underlying synaptic structure is represented in Figure 8(b). After approximately 200ms of activation a cell-assembly is retrieved in 3-cycle DS. At 300ms we increase inhibition to shut off the first memory before activating the second one. The synaptic matrix is shown in Figure 8(b) in a random and an ordered basis. The first memory is encoded by neurons 1 to 100 and the second one by numbers 80 to 180. Note (in the left frame of Figure 8(b)) that the synaptic connections shared by the two cell assemblies encode the second memory. Nevertheless, the first cell assembly can still be retrieved in a distributed synchrony mode. Higher overlaps between the two cell assemblies destroy retrieval of both memories.

It should be noted that this figure displays a retrieval process in which no active synaptic learning took place. In fact, if we allow synaptic learning to occur under the same conditions listed above, the learning process will destroy the segmented synaptic matrix structure and merge the two cell-assemblies. Encoding of many memories using activation by inputs requires well specified protocols to ensure proper allocation of basins of attraction to all memories. An example of how to perform such encoding using the concept of neuronal regulation was demonstrated in Horn *et al.* (1998). The extension of this method to the system of spiking neurons requires further study.

8 Discussion

The asymmetric temporal nature of synaptic learning curves among excitatory neurons, as observed by Markram *et al.* (1997) and Zhang *et al.* (1998), naturally leads to asymmetric, and to some extent antisymmetric, synaptic matrices. This is manifested in our various simulations, starting with Fig. 3, and in our analytic results. The main point that we make in this article is that this asymmetry helps to engrave and stabilize a cyclic firing pattern that we call distributed synchrony.

The system that we have studied contains relatively simple spiking neurons, with pulse-coupled interactions whose temporal structure is specified by delay parameters τ_d . The synaptic efficacies themselves are assumed to be simple numerical coefficients. All these are simplifications introduced in order to single out the one aspect that we wished to study, i.e. the effect of the synaptic learning curve on the evolving firing pattern. It is to be expected that introducing α -functions for synaptic efficacies, and adding activity dependent effects, both on the synaptic level (Markram and Tsodyks (1996) and Abbott *et al.* (1997)) and on the neuronal level (Horn *et al.* (1998) and Turrigiano *et al.* (1998)), will further complicate the temporal structure of the firing patterns.

Our dynamical system led to sustained activity, that we interpret as the neuronal correlate of memory retrieval, at a rate of the order of 100 Hz. This should change once a more biological neural model is employed, e.g. one that incorporates after-hyperpolarization effects. One may then expect to find sustained activity at lower frequencies. Accordingly one can then employ a STDP rule with wider time windows than shown in Fig. 1, corresponding to experimental observations. Once sustained activity is brought down to the range of few tens of Hz, one may expect short-term synaptic depression (Markram and Tsodyks (1996) and Abbott *et al.* (1997)) to be of little consequence.

A further simplification in our model is that only the excitatory-excitatory synapses undergo active learning, with all other synapses remaining constant. Our model includes inhibitory neurons whose role is to provide competition between the excitatory neurons. It may well be that inhibitory neurons undergo different types of STDP, of a symmetric nature in time (see the recent review of Abbott and Nelson (2000)). If this is the case, incorporating such behavior in the model may leave our conclusions in tact.

Our parameter space is quite large. In the absence of closed analytic solutions we were not able to exhaustively map it. DS solutions were found within windows of parameter space, often connected to regions of asynchronous behavior. In many parameter regimes one

could dynamically flow into either DS or asynchrony, and sometimes also into synchronous firing, with different probabilities. In general we have found that low values of τ_s facilitate the creation of a DS cycle. Applying low values of τ_s in the first stage of learning and high values later on is a strategy that may reflect some transient factors involved at the beginning of the process of encoding a new memory. This strategy increases the probability of DS formation.

Clearly the DS mechanism would work best if it is activated in an ordered fashion, rather than letting it emerge spontaneously from global noisy activation of a large set of neurons. One could then envisage the formation of very large cycles, maybe of the type of synfire chains (Abeles (1982)) that show recurrence of firing patterns of groups of neurons with periods of hundreds of ms. The model by Herrmann *et al.* (1995), which realizes synfire chains by combining sets of preexisting patterns into a cycle, can perhaps be tied with such a learning mechanism. Alternatively, if one thinks of the long chains as being formed spontaneously, no semantic meaning should be given to the various elements of the cycle.

It is interesting to speculate whether the DS phenomenon can have any important cognitive role. Bienenstock (1995) has discussed the importance of synfire chains and analyzed the possibility of dynamic binding between chains of equal length. Another intriguing possibility is binding of cell-assemblies that fire with the same overall period but possess different numbers of cycles. In this case different configurations of relative ordering of the subassemblies are possible, each leading to different Hebbian connections that will foster their reoccurrence in future activations. One may thus envisage a mechanism for encoding various combinations of multiple memories, maybe in some hierarchical order with stronger couplings within an assembly and weaker couplings among different assemblies, thus building a rich repertoire of composite memories.

Appendix A Calculating \bar{F} and C

The moments of $F_{ij}(t)$ are calculated assuming the network fires in a stationary manner. In order to extract the relevant moments let us start by rewriting Eq. 5 in a slightly modified manner:

$$F_{ij}(t) = \sum_{k,l} \delta(t - t_i^k) K(t_j^l - t_i^k) , \quad (\text{A.1})$$

where, for the sake of brevity, we united the two δ -functions, whose precise timing is immaterial to the analysis that will be carried out below. Next we note that the spike trains fired by neurons i and j are defined as $S_i(t) = \sum_k \delta(t - t_i^k)$ and $S_j(t) = \sum_l \delta(t - t_j^l)$. In a stationary situation they will correspond to firing rates, or frequencies, ν_i and ν_j . For the problem at hand we assume that these frequencies are the same, $\nu_i = \nu_j = \nu$, and the two spike trains differ by a random phase η whose distribution function will be denoted by $p(\eta)$. For simplicity it will be assumed to be Gaussian with average μ_η and standard deviation σ_η .

Eq. A.1 can be rewritten (see Rieke *et al.* (1997)) as

$$F_{ij}(t) = S_i(t) \int K^*(s) S_j(t-s) ds . \quad (\text{A.2})$$

where $K^*(s) = K(-s)$. Its time averaged value is given by

$$E[F_{ij}] = \nu^2 \int p(x) K^*(x) dx \quad (\text{A.3})$$

while

$$E[F_{ji}] = \nu^2 \int p(x) K^*(-x) dx . \quad (\text{A.4})$$

The last identity follows because if $\eta(t)$ is the phase shift between neurons i and j then the phase shift between the spike trains of j and i is $-\eta(t)$.

Regarding F_{ij} as a random variable determined by the distribution function $p(x)$ we find the following second-order moments:

$$E[F_{ij}^2] = \nu^4 \int p(x) K^{*2}(x) dx , \quad (\text{A.5})$$

and

$$E[F_{ij}F_{ji}] = \nu^4 \int p(x)K^*(x)K^*(-x)dx . \quad (\text{A.6})$$

For a given density function p the means $\mu_{F_{ij}}$ and $\mu_{F_{ji}}$ of F_{ij} and F_{ji} , the standard deviations $\sigma_{F_{ij}}$ and $\sigma_{F_{ji}}$, the covariance $Cov[F_{ij}, F_{ji}]$ and the correlation ρ can be calculated from the expressions derived above.

References

- Abbott, L. F. & Nelson, S. B. (2000), ‘Synaptic plasticity: taming the beast’. *Nature Neuroscience Supplement*, **3**, 1178-1183.
- Abbott, L. F., Sen, K., Varela, J. A. & Nelson, S. B. (1997), ‘Synaptic depression and cortical gain control’. *Science* **275** 220 - 222.
- Abeles, M. (1982), *Local Cortical Circuits*, Springer, Berlin.
- Bienenstock, E. (1995), ‘A model of neocortex’, *Network: Computation in Neural Systems* **6**, 179 – 224.
- Brunel, N. (1999), ‘Dynamics of sparsely connected networks of excitatory and inhibitory spiking neurons’, *Journal of Computational Neuroscience* .
- Gardiner, C. W. (1985), *Handbook of stochastic methods*, 2 edn, Springer-Verlag.
- Golomb, D., Hansel, D., Shraiman, B. & Sompolinsky, H. (1992), ‘Clustering in globally coupled phase oscillators’, *Physical Review A* **45**(6), 3516 – 3530.
- Hansel, D., Mato, G. & Meunier, C. (1995), ‘Synchrony in excitatory neural networks’, *Neural Computation* **7**, 307 – 337.
- Herrmann, M., Hertz, J. & Prügel-Bennet, A. (1995), ‘Analysis of synfire chains’, *Network: Comp. in Neural Systems* **6**, 403 – 414.

- Horn, D., Levy, N. & Ruppin, E. (1998), ‘Memory maintenance via neuronal regulation’, *Neural Computation* **10**, 1 – 18.
- Horn, D., Levy, N., Meilijson, I. & Ruppin, E. (2000), ‘Distributed synchrony of spiking neurons in a Hebbian cell assembly’, in S. A. Solla, T. K. Leen & K.-R. Müller, eds, ‘Advances in Neural Information Processing Systems 12: Proceedings of the 1999 Conference’, MIT Press, pp. 129 – 135.
- Kempler, R., Gerstner, W. & van Hemmen, J. L. (1999), ‘Spike-based compared to rate-based Hebbian learning’, in M. S. Kearns, S. A. Solla & D. A. Cohn, eds, ‘Advances in Neural Information Processing Systems 11: Proceedings of the 1998 Conference’, MIT Press, pp. 125 – 131.
- Markram, H., Lübke, J., Frotscher, M. & Sakmann, B. (1997), ‘Regulation of synaptic efficacy by coincidence of postsynaptic apss and epsps’, *Science* **275**(5297), 213 – 215.
- Markram, H. & Tsodyks, M. (1996), ‘Redistribution of synaptic efficacy between neocortical pyramidal neurons’. *Nature* 382, 807 – 810.
- Rieke, F., Warland, D., de Ruyter van Steveninck, R. & Bialek, W. (1997), *Spikes*, MIT Press. ‘
- Song, S., Miller, K. D., & Abbott, L. F. (2000), ‘Competitive Hebbian learning through spike-timing-dependent synaptic plasticity’, *Nature Neuroscience* **3** 919 - 926.
- Turrigiano, G. G., Leslie, K. R., Desai, N. S., Rutherford, L. C. & Nelson, S. B. (1998), Activity-dependent scaling of quantal amplitude in neocortical neurons. *Nature*, **391** 892–895.
- van Vreeswijk, C. (1996), ‘Partial synchronization in populations of pulse-coupled oscillators’, *Physical Review E* **54**(6), 5522 – 5537.

Zhang, L. I., Tao, H. W., Holt, C. E., Harris, W. A. & Poo, M. (1998), 'A critical window for cooperation and competition among developing retinotectal synapses', *Nature* **395**, 37 – 44.